Sensors & Transducers Journal, Vol. 137, Issue 2, February 2012, pp. 145-154

www.sensorsportal.com

Sensors & Transducers

ISSN 1726-5479

http://www.sensorsportal.com

Electrical and Humidity Sensing Study of Nanocrtsyallite Mg-Cd Ferrites

[a]Ashok B. GADKARI, [b] Tukaram J. SHINDE, [c] Pramod N. VASAMBEKAR

*[a] Department of Physics and Electronics, GKG College, Kolhapur – 416012, (MS) India

[b] Department of Physics, KRP Kanya Mahavidylaya, Isalmpur – 415409, (MS) India

[c] Department of Electronics, Shivaji University, Kolhapur - 416004, (MS) India

[*] Tel.: 09423814704

[*] E-mail: ashokgadkari88@yahoo.com

Received: 15 January 2012 /Accepted: 14 February 2012 /Published: 28 February 2012

Abstract: Nanocrystallite Mg-Cd ferrite samples were prepared by oxalate co-precipitation method. The XRD reveals single phase cubic spinel nature of materials. The crystallite size lies in the range of 27.79 to 30.4 nm. DC electrical resistivity decreases with increasing temperature indicating the semiconductor behavior. The DC electrical resistivity increases and the Curie temperature decreases with increase in cadmium content. All the samples show decrease in resistivity with increase in relative humidity. All the samples are humidity sensitive in low humidity range (40 to70 %). The electrical resistivity of Cd substituted samples decreased by three order of magnitude, when %RH increased from 40%RH to 90%RH. The response and recovery time of all the samples are 200-300 sec. The shorter response time was 240s for composition x = 0.4. *Copyright © 2012 IFSA.*

Keywords: Humidity sensor, Sensitivity, DC resistivity, Activation energy.

1. Introduction

Nanosize magnetic particles have important technological applications. The spinel ferrites have applications ranging from microwave to radio frequencies [1, 2]. The electric and magnetic properties of spinel ferrites are dependent on the type of magnetic ions residing on the tetrahedral A-site and octahedral B-site of the spinel lattice. Magnesium ferrite has partial inverse spinel structure and wide range application due to high resistivity and high Curie temperature [3, 4]. The Curie temperature depends on composition, additives, synthesis method and microstructure. The change in Curie point was observed with composition in $MgFe_2O_4$ ferrites [3]. For many years humidity sensor have been

widely used in many application including storage of food and computer component as well as control of human and laboratory environments [4]. Controlling and monitoring of accurate and reliable estimate of water content are practically essential in various fields, including air quality detection, food, inflammable gas inspection, health care defense, security clinical and biological sectors [5]. In addition research labs and clean room is all environment that are highly affected by moisture levels and require constant monitoring. Thus many scientific and technological efforts have been made in humid sensor, aiming at improving the response/recovery, selectivity, stability for particular use [5,6]. There are many reports that porous material can be used as humidity sensors [7-9]. In recent year, monitoring and auto-controlling of local humidity environmental become important topic in the field of industry, agriculture, military and house hold [9].

It is well-known that many porous metal oxides [10-12] can be used as humidity-sensing materials; the adsorption of water vapor can enhance the surface electrical conductivity and dielectric constant of the metal oxides [13]. It is known that some polycrystalline ferrites [7-9,11,12,15-18] can be use as very good humidity sensor element. One more advantage of using ferrites is their porosity, this being the need for a humidity sensor. Another advantage is their high resistivity which cans changes with about three orders of magnitude with changes in the surrounding humidity. Bagum *et al* [12] also reported $MgCl_2$ doped Cu-Zn ferrites. They observed that the Cu-Zn ferrites with low doping of $MgCl_2$ could be a suitable candidate for humidity sensing. Rezlescu *et al* [15] noticed that the resistivity of La-substituted ferrite is almost insensitive to the humidity. Ni and Mn substituted $MgFe_2O_4$ studied by Rezlescu *et al* [16]. The Mn substituted $MgFe_2O_4$ is used as humidity sensor in relative high range of humidity. Seki *et al* [17] have reported the ferrites utilization as humidity sensors. In a humidity sensitive sensor, the electronic conductivity and carriers concentration changes with the amount of chemisorbed water. Vaingankar *et al* [18] have investigated the humidity sensitivity of electrical properties of Cu-Zn ferrite and they reported that the humidity dependent properties are considerably enhanced by doping this ferrite with $CaCl_2$ and LiCl.

In present communication, we report the DC electrical resistivity, Curie temperature and humidity sensing of nanocrystallite Mg-Cd ferrites prepared by oxalate co-precipitation technique.

2. Experimental

Polycrystalline ferrites with general formula $Mg_{1-x}Cd_x Fe_2O_4$ (x = 0, 0.2, 0.4, 0.6, 0.8 and 1.0) were synthesized by the oxalate co-precipitation method using high purity sulphates. The detail method of synthesis for sample under investigation is reported elsewhere [19]. The co-precipitate obtained was dried and presintered at 700 ^oC for 6 h in air. The presintered powder was milled in an agate mortar with AR grade acetone and sintered at 1050 ^oC for 5 h. The sintered powder was mixed with binder (2% polyvinyl alcohol by weight) and pressed into the pellets of 13 mm diameter by applying pressure of 7 tones/cm^2 under the hydraulic press. The pellets were finally sintered at 1050^oC for 5 h.

The X-ray diffraction (XRD) patterns were obtained at room temperature on Philips PW-3710 X-ray powder diffractometer in the range of 20-80^o using CuK_α radiation (λ= 1.5424 A^o). The crystallite size was calculated by Debye Scherrer's formula. The micrographs of fractured surfaces of the pellets were taken on a scanning electron microscope (JEOL – JSM 6360 model, Japan). The IR absorption spectra of powdered samples were recorded in the range of 350 cm^{-1} to 800 cm^{-1} on Perkin-Elmer FT-IR spectrum one spectrometer using KBr pellet technique.

DC resistivity (ρ) measurements of all the samples were carried out by using two probe method in the temperature range of 300-800^{0}K. The digital picometer model (DPM-111) was used to record current through the samples keeping constant voltage across the sample at room temperature as well as above

Curie temperature. Curie temperature is measured by Loria Sinha method and is also determined from DC resistivity measurement.

The humidity testing of the sensors was conducted using Aditi Associate Model ASC-10 Mumbai make microprocessor controlled humidity chamber. It consists of double wall exterior with made up of steel metal and interior of stainless steel. A flush fitting insulated door has leak proof gasket. The relative humidity was generated by pure water droplets by circulating water in chamber. The sensor element (pellet) about 2mm thickness and 13 mm in diameter were fixed in conducting cell. For good electrical contact silver contacts were made on sensor element. DC voltage is applied across the sensor element with help constant potential voltage source. The resistance of sensor (pellet) was measured by two probe method with a picometer. The measurement was performed at the temperature 27 ^{0}C. The humidity was increased from 40%RH to 90%RH in steps of 10%RH, since it takes around 20-30 minutes for the chamber to reach equilibrium, the readings are taken 30 minutes after a humidity setting has been changed.

3. Results and Discussion

3.1. Synthesis and Characterization

The structural analysis of Mg-Cd ferrite samples under investigations are already reported [19]. The typical XRD pattern of $MgFe_2O_4$ is presented in Fig. 1. All the samples show single phase cubic spinel structure. The average crystallite size of the samples obtained from Debye Scherrer's relationship is in the range 27.79 to 30.40 nm. Typical micrograph of $CdFe_2O_4$ is presented in Fig. 2. The average grain size in the samples is calculated by linear intercept method. It lies in the range of 0.58 μm to 1.2 μm. Typical IR absorption spectra of $Mg_{0.6}Cd_{0.4}Fe_2O_4$ is presented in Fig. 3. It shows two absorption bands (υ_1 and υ_2) in the high frequency range of 555 to 576 cm^{-1} and low frequency range of 431 to 472 cm^{-1} respectively [19].

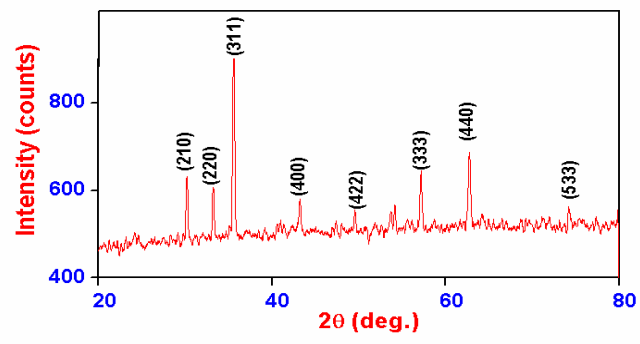

Fig. 1. Typical X-ray diffraction patterns of $MgFe_2O_4$ system (x = 0).

Fig. 2. SEM micrographs of $CdFe_2O_4$ system (x =1).

3.2. DC Electrical Resistivity and Curie Temperature Measurement

The effect of temperature on the DC electrical resistivity (ρ) of $Mg_{1-x}Cd_xFe_2O_4$ ($0 \leq x \leq 1$) has been investigated in the range 300-800 ^{0}K. The variation of logρ against 10^3/ T for all the samples under investigation is plotted in Fig. 4.

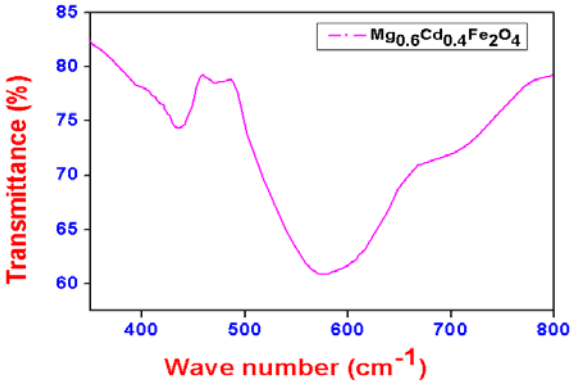

Fig. 3. Typical FT-IR spectra of $Mg_{0.6}Cd_{0.4}Fe_2O_4$ system (x = 0.4).

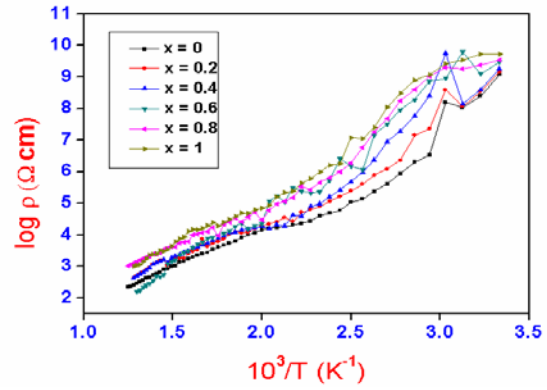

Fig. 4 Variation of log ρ against $10^3/T$ for $Mg_{1-x}Cd_x Fe_2O_4$ system.

It is observed that the electrical resistivity of all the samples decreases with increasing temperature, suggesting the semiconducting nature of the samples. The temperature dependence of resistivity is found to follow the Arrhenius relation [20],

$$\rho = \rho_o e^{(\Delta E/KT)}, \quad (1)$$

where ρ_o is the pre-exponential factor with the dimensions of Ω cm, K is the Boltzmann constant (8.62×10^{-5} eV/K), ΔE- is the activation energy and T- is the absolute temperature. The conduction in ferrites under investigation can be explained on the basis of Verwey *et al* [20] mechanism that involves exchange interaction between the ions of the same element in more than one valence state distributed randomly over crystallographic lattice state. The decrease in DC resistivity of ferrites with increasing temperature is attributed to the increase in the drift mobility of electric carriers, which are thermally activated with increasing temperature. Also the conduction in ferrites is due to hopping of electrons between Fe^{2+} to Fe^{3+} ions at elevated temperature [21, 22]. The number of such pairs depends on sintering condition and amount of reduction of Fe^{2+} to Fe^{3+} at elevated temperature. The resistivity of ferrite is controlled by the Fe^{2+} concentration on B-site. As the transfer of electrons from Fe^{2+} to Fe^{3+} ion occur within the octahedral sites, it does not cause the change in the energy state of the crystal as a result of the transition. It is reported that Cd^{2+} ions prefer the occupation of tetrahedral A- sites [23], Mg^{2+} and Fe^{3+} ions partially occupy the A and B-sites [23, 24]. It is also observed that resistivity of the samples increases with increase in Cd^{2+} content. As the Cd^{2+} content increases the Fe^{3+} ions concentration at A-site decreases. Due to this, the number of Fe^{2+} and Fe^{3+} ions responsible for electric conduction in ferrites decreases at A-site. This causes the reduction in A-A and A-B exchange

interaction. Therefore the ferrite containing appreciable amount of cadmium are characterized by strong B-B exchange interaction [25]. This would affect the activation energy needed for transfer of electron between Fe^{2+} and Fe^{3+} ($Fe^{2+} \leftrightarrow Fe^{3+}$). The replacement of magnesium and iron ion by cadmium ion on A-site increases the concentration of Fe^{3+} and Mg^{2+} on B-site. The magnesium ion on B-site abstracts the electron hopping between the iron ions by blocking the $Fe^{2+} \rightarrow Fe^{3+}$ exchange which increases the resistivity. The conversation of Fe^{3+} to Fe^{2+} ions at the B-sites modifies the conduction due to electron hopping because of the decrease in the number of Fe^{3+} ions and equal increase in the Fe^{2+} ions in the B-sites. Thus resistivity increases. Similar observations have also been reported by Manzen *et al* [25] for the system $Mn_{1-x}Cd_x Fe_2O_4$.

DC electrical resistivity of Zn^{2+} and Cd^{2+}substituted Mg ferrites has been reported by Karche *et al* [3] and Ladgaonkar *et al* [24]. They observed increase in DC resistivity of Mg ferrites with increasing Zn^{2+} and Cd^{2+} concentration of samples prepared by ceramic method. This is attributed due to the increase in porosity, as the result of increase in Zn^{2+} and Cd^{2+} content in Mg ferrite. The high resistivity of the samples under investigation is also attributed due to its smaller grain size [19]. It is also observed that the resistivity of ferrites under investigation is higher than the reported value of resistivity of ferrites prepared by ceramic method [3]. In present investigation the resistivity of ferrites at room temperature lies in the range 1.1×10^8 to 5.5×10^8 Ω cm.

Each sample shows break resistivity versus 1/T plot near Curie temperature which is attributed to the transition from ferri to paramagnetic region. The activation energy has been calculated from the plot of logρ against 10^3/ T. The activation energy (ΔE) in ferri and para regions is presented in Table 1. In all the samples the activation energy in paramagnetic region is greater than that in ferrimagnetic region [26]. The lower activation energy in ferrimagnetic region is attributed to the phase transition or impurity phases [27]. Similar results are also found for others spinel ferrites [3, 28, 29]. This phase transition is known as order to disorder transition. The activation energy decreases with increasing cadmium content in the Mg-Cd ferrites. This change in activation energy for different compositions is attributed to the hopping of polarons. Such decrease in the activation energy on cadmium substituted magnesium ferrite is reported [3]. The substituted cadmium invariably occupies the tetrahedral A-site. This provides increase in the concentration of iron on B-sites resulting decreasing in activation energy.

Table 1. Different parameters estimated form DC resistivity, Curie temperature and humidity sensing of $Mg_{1-x}Cd_xFe_2O_4$ system (x = 0, 0.2, 0.4, 0.6, 0.8 and 1).

Cd^{2+} Content (x)	Crystallite size D (nm)	Humidity Sensitivity S (%)	Response/Recovery time		Activation energy ΔE (eV)		Curie temperature T_c (^{0}K)	
			Response	Recovery	Ferri region	Para region	DC resistivity	Loria Sinha
0.0	29.978	44.56	255	300	0.555	0.995	720	715
0.2	28.434	61.50	250	275	0.469	0.719	660	648
0.4	27.795	64.40	240	256	0.301	0.670	610	613
0.6	29.554	70.65	245	260	0.267	0.450	570	566
0.8	29.069	75.70	235	265	--	0.332	504	502
1.0	30.401	71.60	245	276	--	0.248	--	--

Curie temperatures (T_c) are measured by Loria Sinha [30] method and that observed in DC resistivity measurement are good agreement with each other (Table 1). The Curie temperature of $MgFe_2O_4$ is good agreement with previous report [3, 31]. Fig. 5 shows variation of Curie temperature from DC resistivity and Loria Sinha method with cadmium content. It can be seen that the Curie temperature shows decreasing trend with increasing cadmium concentration. It is known that the T_c depends on A-B interaction (J_{AB}). The decrease in Curie temperature with Cd ions is due to the decrease in A-B

interaction resulting from replacement of Fe^{3+} by Cd^{2+} on tetrahedral A-sites [25]. As mentioned above an increase in Cd^{2+} content causes an increase in lattice constant. This means that the distance between the ions increases, which leads the different A-B interactions to decrease. Also this can be attributed to Cd^{2+} ions having zero magnetic moment at room temperature occupying tetrahedral A-sites and hence resulting in decreased A-B interaction (J_{AB}) between Cd^{2+} and Fe^{3+} ions. Similar results are reported for case of Mg-Cd [3], Mn-Cd [25] and Cd-Co [29] ferrites.

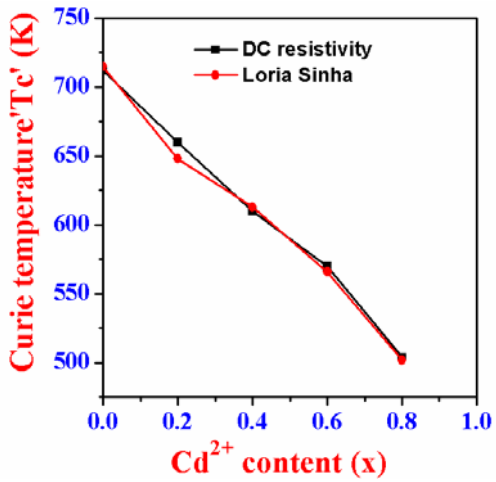

Fig. 5. Variation of Curie temperature with Cd^{2+} content (x) for $Mg_{1-x}Cd_x Fe_2O_4$ system.

3.3. Humidity Sensing

The sensor element with large surface area tends to higher humidity sensitivity, especially in lower humidity range [14]. The substitution of cadmium with magnesium, increases grain size and decreases surface area. These changes in microstructure induced by substitutions seem to lead to an increase or decrease in the amount of physisorbed and condensed water and in the result to a smaller or larger electrical resistivity at same relative humidity. Variation of resistivity with humidity (% RH) of $Mg_{1-x}Cd_xFe_2O_4$ (x = 0, 0.2, 0.4, 0.6, 0.8 and 1) system is shown in Fig. 6. All the samples exhibit a significant decrease in the electrical resistivity in resistivity with an increase in relative humidity from 40 to 90 %. The graph clearly shows that the decrease in resistivity with increase in %RH is very large from 40 to 70 % RH. All the samples are humidity sensitivity in low humidity range of 40 to 70%RH. The resistivity of these elements exponentially decreases with three orders in magnitude according to equation

$$\rho = \rho_0 \, e^{-SRH} \quad , \tag{2}$$

where S is the humidity sensitivity and RH is relative humidity.

It has already been reported in literature [18], that resistivity changes in porous spinel-type oxides with increasing humidity levels occur because of adsorption and capillary condensation of water. At low relative humidity, water adsorption on the sample surface is dominant factor for electronic conduction. Adsorbed water increases the surface electrical conductivity of ceramic due to increased charge carriers, protons in the ceramic/water system [7]. The conductivity is further increased by presence of pores of the sample surface. In the first stage of water adsorption a few water vapor molecules chemisorbs on the grain surfaces by dissociative mechanism to from two surface hydroxyls per molecule. In this chemisorbed layer charge transports occurs by the hopping mechanism [35]. With increasing humidity levels, water is physisorbed on the top of the chemisorbed layer. Conduction

occurs by the Grotthus mechanism [7, 36]. At these high humidity levels the layers of physisorbed water molecules tend to condense in capillary pores. Both Grotthus and hydronium diffusion may occur. This succession of mechanism leads to a rapid increase in conduction (decrease in resistivity) with humidity content.

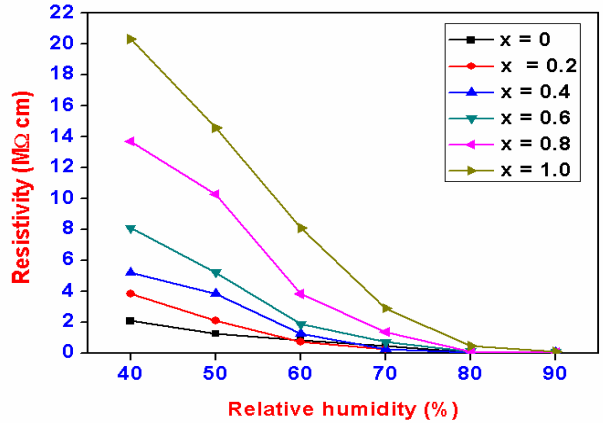

Fig. 6. Variation of resistivity with humidity (%RH) for $Mg_{1-x}Cd_x Fe_2O_4$ system.

The resistivity of the Mg-Cd is very sensitive in a wide humidity range, between 40% and 70% RH. This result might be caused by the increase in porosity which seems to lead to a greater amount of physisorbed water. In consequence, a significant decrease in ρ scale was obtained of about three orders in magnitude [16].

Variation of humidity sensitivity with Cd^{2+} content is presented in Fig. 7.

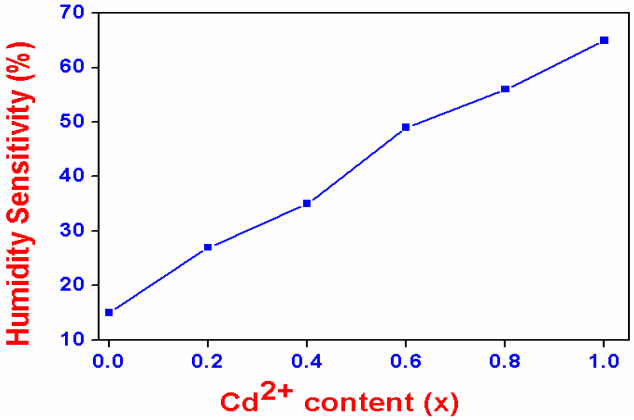

Fig. 7. Variation of humidity sensitivity as function of Cd^{2+} content (x) for $Mg_{1-x}Cd_x Fe_2O_4$ system.

From this figure, it is observed that the sensitivity of all the samples increases with increase in Cd^{2+} content which is attributed to increase in porosity. The ferrite materials are porous in nature and have surface oxygen atoms which essentially arise due to the sample preparation technique. When the material adsorbs humidity, its resistivity decreases due to the increase of charge carriers, protons, in the ferrite and water system [32]. The adsorption of water on the surface of the material leads to the dissociation of hydrogen ions. These hydrogen ions bonded with the surface lattice oxygen atom, forms the hydroxyl groups [33] as shown in the equation

$$H^+ + O_o \leftrightarrow [OH]^- \tag{3}$$

where O_o - corresponds to oxygen at lattice sites. The hydroxyl groups thus produced are bonded with the lattice iron atoms and liberate the free electrons [7].

$$[OH]^- + Fe \leftrightarrow [OH - Fe] + e^- \tag{4}$$

Thus conductivity increases with increase in humidity because of the production of free electrons. Sensitivity of humidity sensor has been defined as the change in resistivity ($\Delta\rho$) of sensing element per unit change in relative humidity (%RH). The sensitivity is calculated by slope of ρ versions %RH curves as given in equation (1). All the samples are humidity sensitive in low humidity range of 40 to 70 % RH and insensitive to humidity at high range of 70 to 90% RH. The sensitivity lies in range of 44 to 76%. Similar results of dc resistivity of $Zn_{0.8}Cu_{0.2}F_2O_4$ doped with $CaC1_2$ and LiCl are found to decrease with increase in %Relative humidity from 45 % to 60 % RH [34].

The response and recovery time of resistivity to change in relative humidity 40 to 90 % for Mg-Cd ferrite is shown in Fig. 8. The response time of the resistivity to the humidity change is about 235 – 300 seconds for all samples. We think that the materials investigated are promising materials for use in humidity controlling devices in a relatively low range of humidity, taking in account the low cost and high durability [18, 35]. However, the response time is not yet a satisfactory value so that further investigations should be directed to the shortening of the response time without any decrease in humidity-sensitivity. The response time of $MgFe_2O_4$ is of about 255 s to attain a steady state value of the resistivity, whereas the response time for $Mg_{0.6}Cd_{0.4}Fe_2O_4$ is shorter, of about 240 s. These results may suggest that the adsorption or desorption rate of water vapors is controlled by the diffusion rate of these through the micropores which in its turn is dependent on the pore size distribution. Large micropores above 0.5 μm are necessary for rapid response to humidity changes. The $MgFe_2O_4$ element, which has a great number of micropores, showed a longer response time to humidity changes [39].

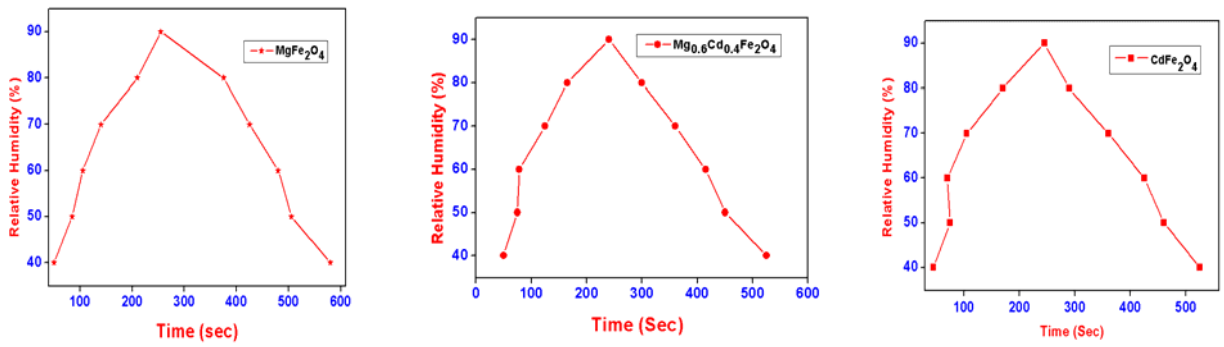

a) $MgFe_2O_4$ b) $Mg_{0.6}Cd_{0.4}Fe_2O_4$ c) $CdFe_2O_4$

Fig. 8. Humidity response and recovery characteristics of $Mg_{1-x}Cd_xFe_2O_4$ system (x = 0, 0.4 and 1).

4. Conclusions

High resistivity nanocrystalline Mg-Cd ferrites can be prepared by oxalate co-precipitation method at low sintering temperature. The crystallite size of the samples varies from 27.79 nm to 30.40 nm range. Dc resistivity decreases with temperature and increases with Cd^{2+} concentration. DC resistivity and Curie temperature are higher than that obtain from ceramic method. Activation energy in paramagnetic

region is higher than that of ferromagnetic region. All the samples show decrease in resistivity with increase in relative humidity. All the samples are humidity sensitive in low humidity range of 40 to 70%RH. The humidity sensitivity increases with increase in Cd^{2+} content. The electrical resistivity of Cd substituted samples decreased by three orders of magnitude, when %RH increased from 40% to 90%RH. The response and recovery time of all the samples are 200-300 sec. The shorter response time was measured to be 240s for the composition x= 0.4.

References

[1]. J. Smit and J. Verweel, Ferrites at radio frequencies, *Mc Graw-Hill,* New York, 1971.

[2]. S. L. Blum, J. E. Zneimer and H. Zlotnick, Effect of ceramic parameters on microwave properties of Nickel ferrite, *J. Am. Ceram. Soc.,* Vol. 40, Issue 5, 2006, pp. 143-149.

[3]. B. R. Karache, B. V. Khasbardar and A. S. Vaingankar, X-ray, SEM and magnetic properties of Mg-Cd ferrites, *J. Magn. Magn. Mater.,* Vol. 168, Issue 24, 1997, pp. 292-296.

[4]. H. Aria, T. Seiyma, Humidity Sensors: A Comprehensive Survey, 3rd ed, W. Gopal, J. Hesse and J. N. Zemel, *Weinheim VCH*, 1992, pp. 981-1012.

[5]. Y. Feng, S. Wang, B. Feng, Y. He, T. Zhang, Development of an auto test system for humidity sensors, *Sens. Actuators A,* Vol. 152, Issue 2, 2009, pp. 104-109.

[6]. B. Ostrick, R. Pohle, M. Fleischer, H. Heixner, Tin in work function type sensors: a stable ammonia sensitive material for room temperature operation with low humidity cross sensitivity, *Sens. Actuators B: Chem.*, Vol. 68, Issue 1-3, 2000, pp. 234-239.

[7]. K. Arshaka, K. Twomej, D. Egan, A ceramic thick film humidity sensor based on MnZn ferrite, *Sensors*, Vol. 2, Issue 2, 2002, pp. 50-61.

[8]. T. Nitta, Z. Terada, S. Hayakawa, Humidity-sensitive electrical conductance of $MgCrO_4$-TiO_2 porous ceramics, *J. Am. Soc. Vol.*, 63, Issue 5-6, 1979, pp. 295-300.

[9]. G. Gummano, G. Montesperelli, P. Nanziante, E. Traversa, Humidity-sensitive electrical response of sintered $MgFe_2O_4$, *J. Mater. Sci.*, Vol. 28, Issue 22, 1993, pp. 6195-6198.

[10]. L. Hongxia, S. Zhiming, L. Hongwei, Humidity sensing properties of La^{3+}/Ca^{3+} -doped TiO_2 - 20% wt. % SnO2 thin film derived from sol-gel method, *J. Rare Earths,* Vol. 28, Issue 1, 2010, pp. 123-127.

[11]. N. Rezlescu, E. Rezlescu, P. D. Popa, F. Tudorache, A model of humidity sensor with A Mg based ferrite, *J. Optoelect. Adv. Mater.*, Vol. 7, Issue 2, 2005, pp. 907-910.

[12]. N. Begum, M. A. Gafur, A. H. Bhuiyan, D. K. Saha, $MgCl_2$ doped $Cu_xZn_{1-x}Fe_2O_4$ ferrite humidity sensors, *Phys. Status Solidi A*, Vol. 207, Issue 4, 2010, pp. 986-992.

[13]. H. Arai, S. Ezaki, Y. Shimizu, O. Shippo, T. Seiyama, in *Proceedings of the International Meeting on Chemial Sensors*, 1983, pp. 393.

[14]. J. H. Anderson, G. A. Parks, The electrical conductivity of silica gel in the presence of adsorbed Water, *J. Phys. Chem.*, Vol. 72, Issue 1968, pp. 3362-3368.

[15]. E. Rezlescu, N. Rezlescu, F. Tudorache, P. D. Popa, On the effects of La^{3+} and Ga^{3+} ions in MgCu ferrite humidity–sensitive electrical conductance, *J. Magn. Magn. Mater.*, Vol. 272-276, 2004, pp. 1821-1822.

[16]. E. Rezlescu, N. Rezlescu, P. D. Popa, Microstructure and Humidity-sensitive properties $MgFe_2O_4$, ferrite with Ni and Mn substitutions, *Phys. Stat. Sol.*, Vol. 1, Issue 120, 2004, pp. 3636–3639.

[17]. K. Seki, J. I. Shida, H. Murakami, *IEEE Transactions on Instrum and Measurements*, Vol. 37, 1988. pp. 3.

[18]. A. S. Vaingankar, S. G. Kulkarni, and M. S. Sagare, Humidity sensing using soft ferrites, *Proc. 7th Int. Conf. on Ferrites,* Bordeaux, France, 3-6 September 1996, *J. Phys.*, IV, Vol. 7, 1997, pp. C1 155-156.

[19]. A. B. Gadkari, T. J. Shinde, P. N. Vasambekar, Structural and magnetic properties of nanocrystalline Mg-Cd prepared by oxalate co-precipitation method, *Mater. Sci. Mater. Elec.*, Vol. 21, Issue 1, 2009, pp. 96-103.

[20]. E. J. Verwey, J. H. de Boer, Cation arrangement in few oxides with crystal structure of the spinel type, *Rec. Trav. Chim. Phys. Bas.*, Vol. 55, Issue 6, 1936 pp. 531-540.

[21]. B. Vishwanathan, V. R. K., Murthy, Ferrites material science and technology, *Narosa Publication House*, New Delhi, 1990.

[22]. C. B. Kolekar, P. N. Vasambekar, A. S., Vaingankar, Structural and dc electrical resistivity study of Gd^{3+} substituted Cu-Cd ferrites, *J. Magn. Magn. Mater.*, Vol. 138, Issue 1-2, 1994, pp. 211-215.

[23]. A. A. Mostfa, G. A. El-Shobaky, E. Girgis, Effect of ZnO doping on structural and magnetic properties of $CdFe_2O_4$, *J. Phys. D: Appl. Phys.,* Vol. 39, Issue 1, 2006, pp. 2007.

[24].B. P. Ladgaonkar, P. N. Vasambekar, A. S. Vaingankar, Structural and DC electrical resistivity study of Nd^{3+} substituted Zn-Mg ferrites, *J. Mater. Sci. Letts.*, 19, Issue12, 2000, pp. 1375-1377.
[25].S. A. Manzen, A. E. A. El-Rahiem, B. A. Sabrah, The structural and electrical conductivity of Mn-Cd ferrite, *J. Mater. Sc.*, Vol. 22, Issue 12, 1987, pp. 4177-4180.
[26].S. Mishra, K. Kundu, K. C. Barick, D. Bahudu, D. Chakaravarty, Preparation of nanocrystalline $MnFe_2O_4$ by doping of Ti^{4+} ions using solid state reaction route, *J. Magn. Magn. Mater.*, Vol. 307, Issue 2, 2006, pp. 222-226.
[27].N. Rezlescu, E. Rezlescu, C. Pasaicu, M. L. Craus, Comparison of the effect of TiO_2 and R_2O_3 substitution in a high frequency nickel zinc, *J. Magn. Magn. Mater.*, Vol. 136, Issue 3, 1994, pp. 319- 326.
[28].V. K. Nikumbh, A. V. Nagawade, G. S. Gugale, M. G. Chaskar, A. P. Bakare, The formation, structural, electrical magnetic and Mossbauer properties of ferrispinels $Cd_{1-x}Ni_xFe_2O_4$, *J. Mater. Sci.*, Vol. 37, Issue 3, 2002, pp. 637-647.
[29].P. N. Vasambekar, C. B. Kolekar, A. S. Vaingankar, Crystallographic and dc electrical resistivity study of Cd-Co and Cr^{3+} substituted Cd-Co ferrites, *J. Mater. Sci: Mater. Elec.*, Vol. 10, Issue 9, 1999, pp. 667-671.
[30].K. K. Loria, A. P. B. Sinha, *Indian J. Pure Appl. Phys.*, Vol. 1, Issue 2-3, 1963, pp. 115-165.
[31].R. V. Upadhyay, S. N. Rao, R. G. Kulkarni, Yafet-Kittel type magnetic ordering in Mg-Cd ferrites, *Mat. Letts.*, Vol. 3, Issue 7-8, 1985, pp. 273-277.
[32].X. Q. Liu, S. W. Tao, Y. S. Shen, Preparation and characterization of nanocrystalline α–Fe_2O_3 by sol-gel process, *Sens. Actuators B: Chem.*, Vol. 40, 1997, p. 161.
[33].K. Suri, S. Annapoorni, A. K. Sarkar, R. P. Tandon, Gas and humidity sensors based on iron-oxide-polyprrole nanocomposite, *Sens. Actuators B: Chem.*, Vol. 81, Issue 2-3, 2002, pp. 277-282.
[34].A. Y. Lipare, Ph. D. Thesis, *Shivaji University,* Kolhapur, 2000.
[35].Y. Shimzu, H. Arai, T. Seiyama, Theoretical studies on the impedance-humidity characteristics and ceramic humidity sensors, *Sensors and Actuators,* Vol. 7, Issue 1, 1985, pp. 11-22.
[36].N. Rezlescu, E. Rezlescu, F. Tudorache, P. D. Popa, MgCu nanocrystalline ceramic with La^{3+} and Y^{3+} ionic substitutions used as humidity sensors, *J. Magn. Magn. Mater.*, Vol. 290-291, Issue 2, 2005, pp. 1001-1004.
[37].N. Rezlescu, E. Rezlescu, C. L. Sava, F. Tudorache, P. D. Popa, Effect of some ionic substitutions on sintering, structure and humidity sensitivity of MgCu ferrite, *Phys. Stat. Sol.*, (a), Vol. 201, Issue 1, pp. 2004, pp. 17-25.
[38].T. Seiyama, N. Yamazoe, H. Arai, Ceramic humidity sensors, *Sens. Actuators,* Vol. 4, 1983, pp. 85-96.
[39].N. Rezlescu, E. Rezlescu, C. Doroftei, P. D. Popa, Structure and humidity sensitive electrical properties of Sn^{4+} and Mo^{6+} substituted Mg ferrite, *Sens. Actuators B: Chem.*, Vol. 115, Issue 2, 2006, pp. 589-595.
